Journal of Cellular and Molecular Medicine
A JOURNAL OF TRANSLATIONAL MEDICINE

J. Cell. Mol. Med. Vol 16, No 1, 2012 pp. 83-95

IGF-1 deficiency resists cardiac hypertrophy and myocardial contractile dysfunction: role of microRNA-1 and microRNA-133a

Yinan Hua [a], Yingmei Zhang [a, b], Jun Ren [a, *]

[a] *Division of Pharmaceutical Sciences & Center for Cardiovascular Research and Alternative Medicine, University of Wyoming College of Health Sciences, Laramie, WY, USA*
[b] *Department of Cardiology, Xijing Hospital, Fourth Military Medical University, Xi'an, China*

Received: October 6, 2010; Accepted: January 28, 2011

Abstract

This study was designed to examine the impact of insulin-like growth factor-1 (IGF-1) deficiency on abdominal aortic constriction (AAC)-induced cardiac geometric and functional changes with a focus on microRNA-1, 133a and 208, which are specially expressed in hearts and govern cardiac hypertrophy and stress-dependent cardiac growth. Liver-specific IGF-1-deficient (LID) and C57/BL6 mice were subject to AAC. Echocardiographic and cardiomyocyte function were assessed 4 wks later. Haematoxylin and eosin staining was used to monitor myocardial morphology. Western blot and real-time PCR were used to detect protein and miR expression, respectively. Neonatal rat cardiomyocytes (NRCMs) were transfected with miRs prior to IGF-1 exposure to initiate cell proliferation. Immunohistochemistry and [^{3}H] Leucine incorporation were used to detect cell surface area and protein abundance. C57 mice subject to AAC displayed increased ventricular wall thickness, decreased left ventricular end diastolic and end systolic dimensions and elevated cardiomyocyte shortening capacity, all of which were attenuated in LID mice. In addition, IGF-1 deficiency mitigated AAC-induced increase in atrial natriuretic factor, GATA binding protein 4, glucose transporter 4 (GLUT4) and Akt phosphorylation. In contrast, neither AAC treatment nor IGF-1 deficiency affected glycogen synthase kinase 3β, mammalian target of rapamycin, the Glut-4 translocation mediator Akt substrate of 160 kD (AS160) and protein phosphatase. Levels of miR-1 and -133a (but not miR-208) were significantly attenuated by AAC in C57 but not LID mice. Transfection of miR-1 and -133a obliterated IGF-1-induced hypertrophic responses in NRCMs. Our data suggest that IGF-1 deficiency retards AAC-induced cardiac hypertrophic and contractile changes *via* alleviating down-regulation of miR-1 and miR-133a in response to left ventricular pressure overload.

Keywords: cardiac hypertrophy • IGF-1 • myocardial contraction • microRNA

Introduction

Myocardial compensation in response to pressure overload involves a complex process of ventricular remodelling. Although cardiac hypertrophy is usually deemed an adaptive process to compensate the initial stress, sustained hypertrophic changes are maladaptive, resulting in certain devastating cardiac pathologies including congestive heart failure, stroke and sudden death [1, 2]. Cellular changes of cardiac hypertrophy are characterized by increased cardiomyocyte volume, expression of foetal gene and protein synthesis associated with the activation of a variety of cell signalling cascades [1–3]. In particular, calcineurin-nuclear factor of activated T-cells [4], phosphoinositide 3-kinase (PI-3K)/Akt/glycogen synthase kinase 3 (GSK-3) [5, 6], myocyte enhancer factor-2/histone deacetylases [7, 8], G protein-coupled receptors [9] and mitogen-activated protein kinase [10] are among the major signalling molecules governing cardiac hypertrophic response.

Insulin-like growth factor (IGF)-1 is an important growth factor for survival, proliferation and differentiation in the heart [11]. McMullen and colleagues reported that IGF-1 receptor mediates physiological cardiac growth in a PI-3K-dependent manner. This finding challenges the classical viewpoint of IGF-1 being a potential candidate for the treatment of heart failure [12]. However, the precise role of IGF-1 in the regulation of cardiac function and

*Correspondence to: Dr. Jun REN,
Center for Cardiovascular Research and Alternative Medicine,
University of Wyoming College of Health Sciences,
Laramie, WY 82071, USA.
Tel.: (307)-766–6131
Fax: (307)-766–2953
E-mail: jren@uwyo.edu

doi: 10.1111/j.1582-4934.2011.01307.x

© 2011 The Authors
Journal of Cellular and Molecular Medicine © 2011 Foundation for Cellular and Molecular Medicine/Blackwell Publishing Ltd

geometry under both physiological and pathological conditions is still debatable. Therefore this study was designed to determine the role of IGF-1 deficiency in a murine model of pressure overload-induced cardiac hypertrophy. Given that cardiac hypertrophy has been reported to be governed by microRNA-1, -133a and -208 [13, 14], levels of these miRs were examined in hypertrophic hearts induced by abdominal aortic constriction (AAC). MiRs are a group of non-coding, small RNAs to negatively control the post-transcriptional gene expression [15]. Approximately one third of the mammalian genomes are regulated by miRs with a high tissue specificity [16]. For example, miR-1, miR-133a, miR-206 and miR-208 appear to be muscle specific, whereas miR-1 and miR-133a are unique regulators for cardiac hypertrophy [17, 18]. In an effort to elucidate the cellular machineries behind IGF-1 deficiency and pressure overload-induced myocardial alterations, if any, special attempt was made towards the post-IGF-1 receptor signalling molecule Akt, its downstream targets mammalian target of rapamycin (mTOR) and GSK-3β, as well as protein phosphatase (reciprocally correlated with Akt phosphorylation), all of which are pivotal in the maintenance of cardiac structure and function [19–21]. Given that Akt may phosphorylate Akt substrate of 160KD (AS160) to initiate glucose transport by glucose transporter-4 (GLUT-4) [22], phosphorylation of AS160 and GLUT-4 expression were also monitored in myocardium following pressure overload.

Materials and methods

Experimental animals and AAC

All animal procedures were approved by our Institutional Animal Use and Care Committee (Laramie, WY, USA) and were in accordance with the NIH standard. In brief, the liver-specific IGF-1-deficient (LID) mice on a mixed C57BL/6, FVB/N, and 129sv background were generated using the Cre/loxP system. In order to determine the IGF-1/loxP transgene, genomic DNA was isolated from tail clips using a Quick extraction and amplification kit (BioPioneer, San Diego, CA, USA). To test the presence of Cre transgene (*i.e.* liver-specific IGF-1 gene knockout), Cre-5′ and Cre-3′ primers were used, which yielded a 0.6 kb band for the Cre transgene. Mice homozygous for IGF-1/loxP carrying the albumin-Cre transgene were crossed. The offspring genotyping was executed using a double PCR strategy. To identify the genotype of IGF-1/loxP, primers of insulinoma-associated (IA)6, IA8 and inhibitor of DNA binding (ID)3 were used for PCR reaction. Mice which yield one 0.4 kb band were negative for IGF-1/loxP whereas those with one 0.2 kb band are positive. The presence of both 0.4 and 0.2 kb bands denoted heterozygous IGF-1/loxP. Adult female mice positive for IGF-1/loxP and Cre transgenes were used as LID and C57BL/6 served as control [23, 24]. To create cardiac hypertrophy, mice were anesthetized (Phenobarbital sodium, 50 mg/kg) and placed in a supine position. Abdomen was opened under the sterilized condition. Abdominal aorta at the suprarenal level was dissected free of surrounding adventitial adipose tissues and muscles. The aorta between the celiac and superior mesenteric arteries was constricted by a 6–0 silk suture ligature to yield a ~33% narrowing of luminal diameter. Sham operation included all procedures except the suture ligature. Operative incisions were sutured and mice were allowed to recover on warm pads [25]. Four weeks following operation, mice were used for experimentation.

Echocardiographic evaluation

Mice were anesthetized (Avertin 2.5%, 10 μl/g body weight, intraperitoneally). Cardiac function was evaluated using a 2D guided M-mode echocardiography equipped with a 15–6 MHz linear transducer. Anterior and posterior wall thickness as well as diastolic and systolic left ventricular dimension was recorded. Fractional shortening was calculated from left ventricular end diastolic dimension (LVEDD) and left ventricular end systolic dimension (LVESD) using the equation of (LVEDD – LVESD)/LVEDD [26].

Cardiomyocyte isolation and mechanics

Mouse cardiomyocytes were isolated using Liberase as described [27]. Mechanical properties of myocytes were assessed using an IonOptix™ soft-edge system (IonOptix, Milton, MA, USA). Cardiomyocytes were superfused (~2 ml/min. at 25°C) with a Krebs-Henseleit-bicarbonate (KHB) buffer containing 1 mM $CaCl_2$ while being field stimulated at 0.5 Hz unless otherwise stated. Cell shortening and relengthening were assessed using peak shortening (PS), time-to-PS (TPS), time-to-90% relengthening (TR_{90}) and maximal velocities of shortening/relengthening ($\pm dL/dt$). Myocyte yield was ~75% which was not affected by IGF-1 deficiency or surgery. Only rod-shaped cells with clear edges were selected for mechanical and intracellular Ca^{2+} studies.

Intracellular Ca^{2+} transients

A cohort of myocytes was loaded with fura-2/acetoxymethyl ester (AM) (0.5 μM) for 15 min., and fluorescence intensity was recorded with a dual-excitation fluorescence photomultiplier system (IonOptix). Cells were exposed to light emitted by a 75W lamp and passed through either a 360- or a 380 nm filter, while being stimulated to contract at 0.5 Hz. Fluorescence emissions were detected between 480 and 520 nm, and qualitative change in fura-2 fluorescence intensity (FFI) was inferred from the FFI ratio at the two wavelengths (360/380). Fluorescence decay time (single or bi-exponential decay) was calculated as an indicator of intracellular Ca^{2+} clearing [27].

Histopathological analysis

Ventricular tissues were collected and fixed in 10% formalin for 24 to 48 hrs. The tissues were dehydrated through serial alcohols, cleared in xylenes, and then embedded in paraffin. Paraffin sections were cut to 5 μm thickness and stained with haematoxylin and eosin as described [27]. Cardiomyocyte hypertrophy was quantitated by measuring the diameter of 30 randomly sectioned (longitudinal) cardiomyocytes per microscopic field.

Western blot analysis

Protein was extracted using a Radio-Immunoprecipitation Assay (RIPA) lysis buffer. Equal amounts (25 μg protein/lane) of lysates were separated on 7–12% SDS-PAGE and transferred onto nitrocellulose membranes. Membranes were blocked for 1 hr in using 5% non-fat milk in Tris-buffered saline with Tween (TBST) and incubated overnight at 4°C with the anti-atrial natriuretic factor (ANF), anti-GATA binding protein 4 (GATA4), anti-Akt, anti-pAkt, anti-GSK-3β, anti-pGSK-3β, anti-mTOR, anti-pmTOR, anti-pAS160, anti-GLUT4, anti-PP2AA, anti-PP2AB, anti-PP2Cα and anti-α-tubulin (loading control) antibodies. All antibodies

© 2011 The Authors
Journal of Cellular and Molecular Medicine © 2011 Foundation for Cellular and Molecular Medicine/Blackwell Publishing Ltd

were from Cell Signaling (Boston, MA, USA) or Santa Cruz (Santa Cruz, CA, USA). Following incubation with the primary antibodies, membranes were incubated with an anti-rabbit IgG horseradish peroxidase (HRP)-linked antibody for 1 hr at room temperature. Immunoreactive bands were detected by enhanced chemiluminescence autoradiography by molecular imager Gel Doc XR+ System (Bio Rad, Hercules, CA, USA) [27].

MiR extraction and quantitative real-time PCR analysis

Total RNA containing miR was extracted using a *mir*Vana™ miR isolation kit (Ambion, Inc., Austin, TX, USA). The quality and concentration of purified RNA was detected by the SmartSpec Plus Spectrophotometer (Bio Rad). The total RNA containing miR was used for the quantitative real-time PCR (qRT-PCR) analysis. A total of 20 ng of total RNA containing miR was reverse-transcribed individually with a *mir*Vana™ qRT-PCR miR detection kit (Applied Biosystems, Foster City, CA, USA) using the specific reverse transcribed primers for miR-1, miR-133a and miR-208. Then the cDNA from miRs were used for the PCR assay based on the instruction of the manufacturer, specific primers for miR-1, miR-133a and miR-208 (Applied Biosystems) were used. Relative gene expression was normalized by U6 gene expression [28].

Neonatal rat cardiomyocytes (NRCMs) culture and transfection

Given the technical difficulty and poor transfection efficacy of Lipofectamine transfection in mouse cardiomyocytes, NRCMs were used instead. Cardiomyocytes were isolated from 1- to 2-day-old Sprague-Dawley rats [29]. In brief, hearts were dissected, washed and minced in PBS. Tissues were dispersed in 2.5% trypsin (GIBCO, Carlsbad, CA, USA). After centrifugation, cells were resuspended in DMEM (GIBCO) containing 10% foetal bovine serum (GIBCO) and were plated in culture flask. After 2 hrs, non-attached cells were plated in collagen I-coated culture plates or chamber slides. NRCMs (80% confluency) were transfected with the Pre-miR™ rno-miR-1 and Pre-miR™ rno-miR-133a precursors as well as Cy™3 dye-labelled Pre-miR™ negative control (Ambion, Foster City, CA, USA) using the Lipofectamine™ LTX and Plus Reagent (Invitrogen). A cohort of transfected cells were treated with IGF-1 (30 ng/ml) for 48 hrs before cells were collected for further analysis [30].

NRCM surface area measurement

After transfection with miRs and treatment with IGF-1, NRCMs were rinsed and fixed for 15 min. in 4% paraformaldehyde at room temperature. Cells were washed and permeabilized with 0.2% Triton X-100 in PBS for 15 min. at room temperature, followed by three additional washed with PBS. The cells were blocked with 5% bovine serum albumin for 30 min. prior to incubation with an antibody against muscle specific α-actin at 4°C overnight. The cells were then incubated with a goat anti-rabbit IgG-fluorescein isothiocyanate (FITC) antibody at 37°C for 60 min. Following four rinses with PBS, cells were stained with propidium iodide (1 mg/ml) for 30 min. at 37°C and were viewed using a Nikon Eclipse TE300 microscope (Nikon, Tokyo, Japan) with a Cascade cooled charge-coupled device digital camera (Roper Scientific, Inc., Tucson, AZ, USA). Areas of NRCMs were measured by the NIH ImageJ software using images of myocytes stained with the anti-α-actin antibody [31].

[^{3}H] Leucine incorporation

NRCMs transfected with miRs were treated with IGF-1 (30 ng/ml) for 24 hrs prior to incubation with [^{3}H] leucine (1.0 μCi/ml) for another 24 hrs. Cells were then washed with PBS, incubated with 10% trichloroacetic acid for 20 min. at 4°C and lysed with 0.5 M NaOH overnight. The precipitate was determined by scintillation counting [32].

Statistical analysis

Data were presented as mean ± S.E.M. Statistical analysis was performed with ANOVA followed by a Tukey *post hoc* test using the SigmaPlot software (Jandel Scientific, San Rafael, CA, USA). A *P*-value less than 0.05 was considered statistically significant.

Results

General features and echocardiographic properties

The LID mice weighed significantly less than the age-matched C57 mice, as reported [33]. However, the heart, liver and kidney weights and the organ-to-body weight ratio (with the exception of liver) were not significantly different between LID and C57 mice. The liver size (normalized to body weight) was significantly greater in LID mice compared with C57 mice. Neither AAC nor sham surgery significantly affected body weight in C57 or LID mice. Four weeks after the AAC surgery, the heart weight and heart-to-body weight ratio were significantly increased in C57 mice, the effect of which was ablated or significantly attenuated by IGF-1 deficiency. In contrast, the surgery failed to alter the weight or size of liver and kidney. Echocardiographic examination revealed significantly elevated left ventricular wall thickness, decreased LVEDD and LVESD with unchanged heart rate and fractional shortening in C57 mice following surgery. Although IGF-1 deficiency itself did not affect the echocardiographic parameters measured, it significantly attenuated or nullified AAC-induced cardiac geometric changes without affecting AAC-induced response in heart rate and fractional shortening (Table 1). These data suggest that IGF-1 deficiency ameliorates AAC-induced concentric cardiac hypertrophy.

Cardiomyocyte contractile and intracellular Ca^{2+} properties as well as stimulus frequency response

Neither AAC nor IGF-1 deficiency overtly affected resting cardiomyocyte length. AAC significantly enhanced PS and maximal velocity of shortening/relengthening ($\pm dL/dt$) without affecting TPS and TR_{90} in C57 mice. Interestingly, IGF-1 deficiency

© 2011 The Authors

Journal of Cellular and Molecular Medicine © 2011 Foundation for Cellular and Molecular Medicine/Blackwell Publishing Ltd

Table 1 Biometric and echocardiographic parameters of aged-matched C57 and LID mice subject to AAC

Parameter	C57-sham	C57-AAC	LID-sham	LID-AAC
Body weight (g)	29.3 ± 1.0	29.1 ± 0.5	22.7 ± 0.6*	22.3 ± 0.6*
Heart weight (mg)	151 ± 9	198 ± 11*	142 ± 6	144 ± 7$^{\#}$
Heart/body weight (mg/g)	5.18±0.30	6.82 ± 0.41*	6.27 ± 0.34	6.49 ± 0.29
Heart rate (bpm)	426 ± 41	463 ± 34	416±31	508 ± 13
Liver weight (g)	1.31 ± 0.02	1.29 ± 0.01	1.24 ± 0.01	1.21 ± 0.02
Liver/body weight (mg/g)	45.13 ± 1.02	44.52 ± 0.66	54.86 ± 1.34*	54.55 ± 0.83*$^{\#}$
Kidney weight (g)	0.31 ± 0.01	0.32 ± 0.01	0.25 ± 0.01*	0.24 ± 0.01*$^{\#}$
Kidney/body weight (mg/g)	10.48 ± 0.01	10.87 ± 0.01	10.96 ± 0.01	10.72 ± 0.01
Wall thickness (mm)	0.72 ± 0.09	0.93 ± 0.05*	0.58 ± 0.07	0.71 ± 0.12$^{\#}$
LVEDD (mm)	3.01 ± 0.35	1.85 ± 0.25*	2.72 ± 0.46	2.39 ± 0.34*$^{\#}$
LVESD (mm)	1.66 ± 0.19	1.14 ± 0.11*	1.75 ± 0.28	1.31 ± 0.14*$^{\#}$
Fractional shortening (%)	42.0 ± 4.5	37.3 ± 5.9	38.0 ± 4.3	46.6 ± 5.4

Mean ± S.E.M., $n = 5$–6 mice per group, $^{*}P < 0.05$ *versus* C57-sham group, $^{\#}P < 0.05$ *versus* C57-AAC group.

abolished AAC-induced cardiomyocyte mechanical abnormalities without exerting any obvious effect on cardiomyocyte contractile function by itself (Fig. 1).

Rodent hearts normally contract at high frequencies, whereas our mechanical recording was performed at 0.5 Hz. To evaluate the impact of IGF-1 deficiency or AAC on cardiac contractile function under higher frequencies, we increased stimulus frequency up to 5.0 Hz (300 beats/min.) and recorded the steady-state PS. Cardiomyocytes were initially stimulated to contract at 0.5 Hz for 5 min. to ensure a steady-state before commencing the frequency response. Figure 2A displays a comparable negative staircase of PS with increased stimulus frequency in all groups. These data do not favour a major role of intracellular Ca^{2+} cycling or stress tolerance capacity in IGF-1 deficiency or AAC-associated cardiac mechanical response. To further examine the possible cellular mechanism(s) behind LID or AAC-induced mechanical response, intracellular Ca^{2+} homeostasis was evaluated using the intracellular Ca^{2+} fluorescent dye fura-2. Neither AAC nor IGF-1 deficiency significantly affected intracellular Ca^{2+} handling (including baseline and electrically stimulated intracellular Ca^{2+} (ΔFFI), single and bi-exponential intracellular Ca^{2+} decay rate) (Fig. 2B–F).

Effects of AAC and IGF-1 deficiency on histopathological characteristics of hearts

Without AAC, no gross anatomical and structural differences were noticed in hearts or myocardial samples between C57 and LID groups. AAC triggered cardiac hypertrophy characterized by increased heart size, cardiomyocytes diameter and cardiomyocyte disarray in C57 mice. Although IGF-1 deficiency itself did not affect heart size, cardiomyocyte size and appearance, it negated AAC-induced cardiac hypertrophy (Fig. 3).

Expression of ANF, GATA4, Akt, pAkt, GSK-3β, pGSK-3β, mTOR, pmTOR, pAS160, GLUT4, PP2AA, PP2AB and PP2Cα

To explore the possible mechanism involved in AAC and IGF-1 deficiency-induced myocardial morphological and functional responses, the impact of AAC and IGF-1 deficiency on expression of the cardiac hypertrophy markers ANF and GATA4, the cardiac proliferation factor Akt, and its downstream targets mTOR and GSK-3β, which govern protein synthesis and glycogen synthesis, respectively. Our results indicated that AAC significantly up-regulated ANF and GATA4 expression in C57 mice, the effect of which was attenuated by IGF-1 deficiency. IGF-1 deficiency itself did not significantly affect the expression of ANF and GATA4 (Fig. 4). Furthermore, the pAkt-to-Akt ratio was markedly elevated in C57 but not LID mice following the AAC procedure. Neither AAC nor IGF-1 deficiency overtly affected the pGSK-3β-to-GSK-3β or pmTOR-to-mTOR ratio or the pan expression of GSK-3β and mTOR. Not surprisingly, IGF-1 deficiency itself significantly suppressed the expression of phosphorylation of Akt (Fig. 5).

To explore the mechanism of action behind AAC and IGF-1 deficiency-induced response in Akt activation, expression of GLUT4, the Glut-4 translocation mediator AS160 and protein phosphatases (reciprocally correlated with Akt phosphorylation) including PP2AA, PP2AB and PP2Cα were examined. Neither AAC nor IGF-1 deficiency

© 2011 The Authors
Journal of Cellular and Molecular Medicine © 2011 Foundation for Cellular and Molecular Medicine/Blackwell Publishing Ltd

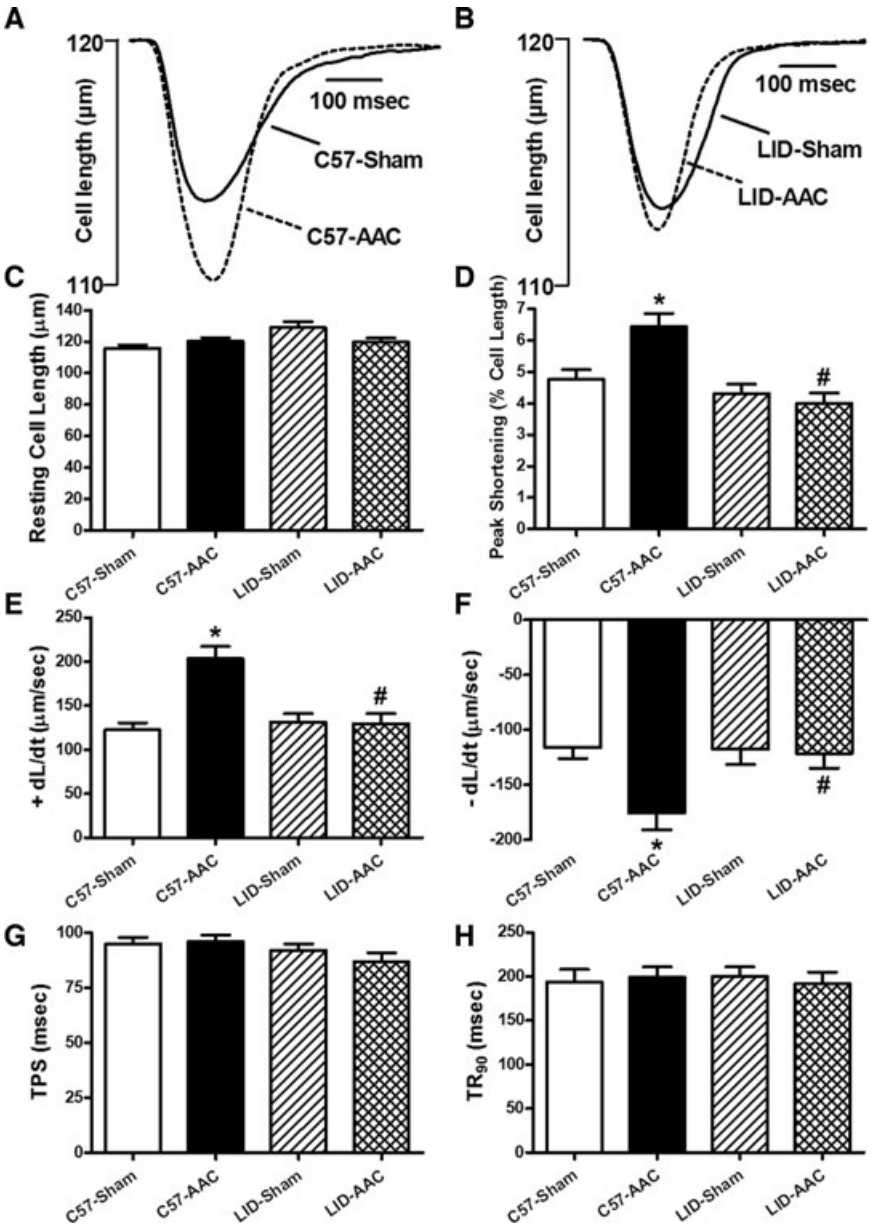

Fig. 1 Cardiomyocyte contractile properties in cells from sham- or AAC-treated C57 and LID mouse hearts. (**A**) Representative cell shortening traces from C57 mice with sham or AAC treatment. (**B**) Representative cell shortening traces from LID mice with sham or AAC treatment. (**C**) Resting cell length. (**D**) PS (normalized to cell length). (**E**) Maximal velocity of shortening ($+dL/dt$). (**F**) Maximal velocity of relengthening ($-dL/dt$). (**G**) TPS and (**H**) TR_{90}. Mean ± S.E.M., $n = 94$–103 cells per group, $^{*}P < 0.05$ *versus* C57-sham group, $^{\#}P < 0.05$ *versus* C57-AAC group.

affected AS160 phosphorylation, PP2AA, PP2AB and PP2Cα levels. However, AAC significantly up-regulated the expression of GLUT4, the effect was significantly attenuated by IGF-1 deficiency. IGF-1 deficiency itself did not affect GLUT4 expression (Fig. 6).

Expression of miR-1, miR-133a and miR-208 in mouse hearts

To demonstrate whether miRs were involved in the IGF-1 deficiency-blunted pressure overload-induced cardiac hypertrophy, the levels of miR-1, miR-133a and miR-208 which are all specific expressed in muscles were detected. After AAC, miR-1 and miR-133a levels were markedly decreased in C57 mice, the effect of which was nullified by IGF-1 deficiency. MiR-208 was also reported to play a role in cardiac hypertrophy [34]. In our study, the expression of miR-208 was not affected by either AAC or IGF-1 deficiency (Fig. 7).

Effect of miRNA-1 and miRNA-133a on IGF-1-induced hypertrophy in NRCMs

To determine the causal–effect relationship between IGF-1 deficiency-induced response in cardiac hypertrophy and miR expression,

© 2011 The Authors

Journal of Cellular and Molecular Medicine © 2011 Foundation for Cellular and Molecular Medicine/Blackwell Publishing Ltd

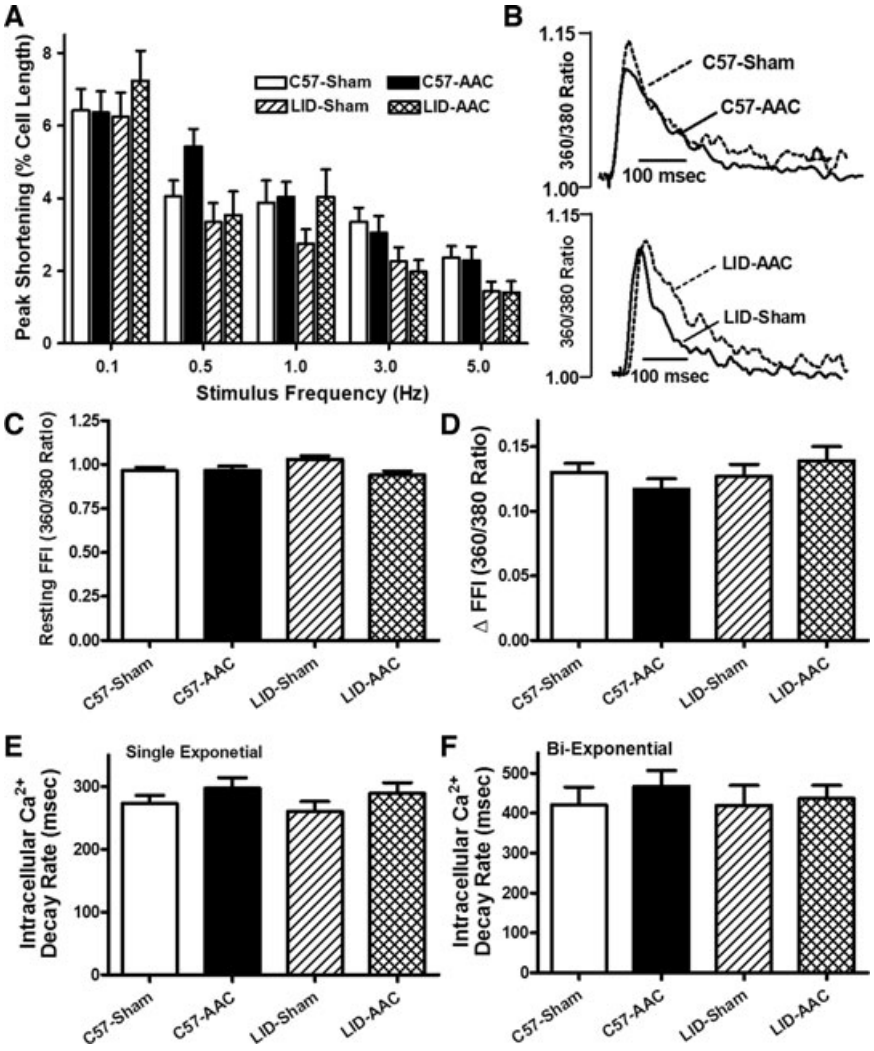

Fig. 2 PS amplitude-stimulus frequency and intracellular Ca^{2+} transient responses in cardiomyocytes from sham- or AAC-treated mouse hearts. (**A**) PS amplitude at various stimulus frequencies (0.1–5.0 Hz). (**B**) Representative intracellular Ca^{2+} transients from sham- or AAC-treated C57 and LID mice. (**C**) Resting FFI. (**D**) Electrically stimulated rise in FFI (ΔFFI). (**E**) Single exponential intracellular Ca^{2+} decay and (**F**) Bi-exponential intracellular Ca^{2+} decay. Mean ± S.E.M., $n = 22$ (**A**) and 80–95 (**C**–**F**) cells per group.

miR-1 and miR-133a were overexpressed in NRCMs to determine if overexpression of miR-1 and miR-133a attenuates the IGF-1-induced hypertrophic response. Intracellular localization of miRNA (Cy3 fluorescence) was confirmed by the presence of Cy3 fluorescence within the overlaid cell FITC fluorescence. Challenge of NRCMs with IGF-1 (30 ng/ml) for 48 hrs triggered cellular hypertrophy as demonstrated by increased cellular size and protein abundance (measured by ^{3}H-leucine incorporation and protein content ratio). Overexpression of both miR-1 and miR-133a markedly suppressed IGF-1-induced hypertrophic response (both cell size and ^{3}H-leucine incorporation) compared with the IGF-1 treatment group (Fig. 8). These results have provided compelling evidence that IGF-1-induced cardiac hypertrophic response is mediated through down-regulation of miR-1 and miR-133a.

Discussion

The salient findings of our study depicted that AAC elicits overt concentric cardiac hypertrophy (increased wall thickness, decreased chamber diameters), preserved fractional shortening and enhanced cardiomyocyte shortening capacity along with unchanged stimulus frequency response and intracellular Ca^{2+} handling properties. The change in cardiac geometry following AAC was accompanied by the increased heart weight, heart-to-body weight ratio and cardiomyocyte diameter, which were mitigated by IGF-1 deficiency. Meanwhile, expression of the cardiac hypertrophy markers ANF and GATA-4 was up-regulated following AAC, the effect of which was attenuated by IGF-1 deficiency. Furthermore, Akt phosphorylation and GLUT4 expression were enhanced whereas phosphorylation of GSK-3β, mTOR and AS160

© 2011 The Authors
Journal of Cellular and Molecular Medicine © 2011 Foundation for Cellular and Molecular Medicine/Blackwell Publishing Ltd

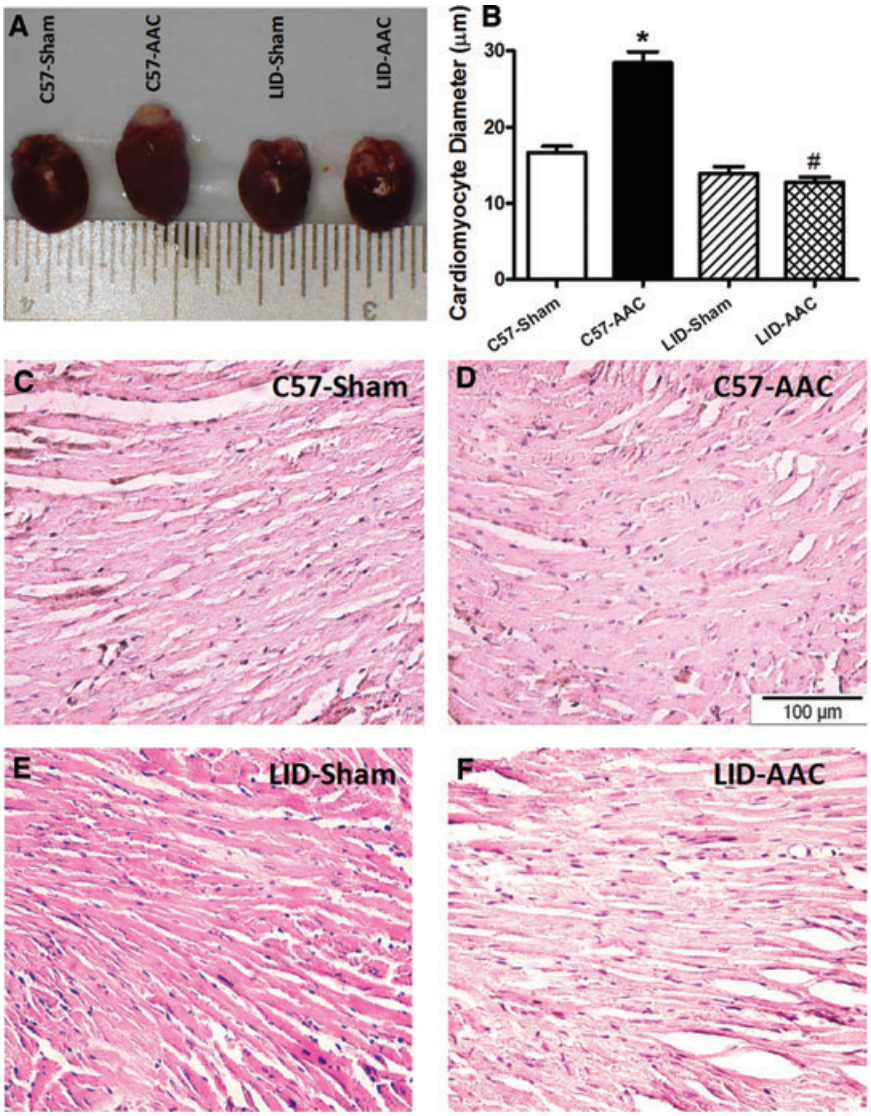

Fig. 3 Whole heart and cardiomyocyte diameter in sham- or AAC-treated C57 and LID mice. (**A**) Representative hearts from sham and AAC-treated C57 and LID mice. (**B**) Pooled cardiomyocyte diameter (longitudinal) from haematoxylin and eosin staining images (400×) and (**C**)–(**F**): haematoxylin and eosin staining from C57-sham, C57-AAC, LID-sham and LID-AAC groups, respectively. Mean ± S.E.M., $n = 12$ fields from three mice (**B**), $^{*}P < 0.05$ *versus* C57-sham group, $^{\#}P < 0.05$ *versus* C57-AAC group.

as well as protein phosphatase levels remained unchanged following AAC. IGF-1 deficiency ablated AAC-induced Akt phosphorylation and GLUT4 up-regulation without affecting the phosphorylation of GSK-3β, mTOR and AS160. These data suggest that IGF-1 deficiency may resist against AAC-induced cardiac hypertrophy through dampened Akt signalling and GLUT4 levels. More importantly, levels of miR-1 and miR-133a but not miR-208 were significantly down-regulated by AAC, the effect of which was blunted by IGF-1 deficiency. Our *in vitro* finding that overexpression of miR-1 and miR-133a abrogate IGF-1-induced cardiomyocyte hypertrophy consolidated the role of miR-1 and miR-133a in IGF-1 deficiency-elicited cardioprotection against pressure overload. Taken together, these observations suggest that IGF-1 deficiency is capable of retarding AAC-induced cardiac hypertrophy and contractile dysregulation, possibly by blunting Akt signalling and rescuing down-regulated miR-1 and miR-133a levels.

Concentric hypertrophy featured by increased cardiomyocyte size is commonly present following pressure overload although dilated cardiomyopathy often represents an end-point for the heart following sustained pathological stresses [35]. In our hand, C57 mice developed overt concentric hypertrophy following AAC procedure as evidence by increased ventricular wall thickness and reduced chamber size. Presence of cardiac hypertrophy is also indicated by heart weight, size, diameter and histological finding. Despite of the preserved myocardial contractility (fractional shortening), cardiomyocyte exhibited significantly enhanced contractile capacity in C57 mice subjected to AAC. This apparent discrepancy between the whole heart and individual cardiomyocytes may be

© 2011 The Authors

Journal of Cellular and Molecular Medicine © 2011 Foundation for Cellular and Molecular Medicine/Blackwell Publishing Ltd

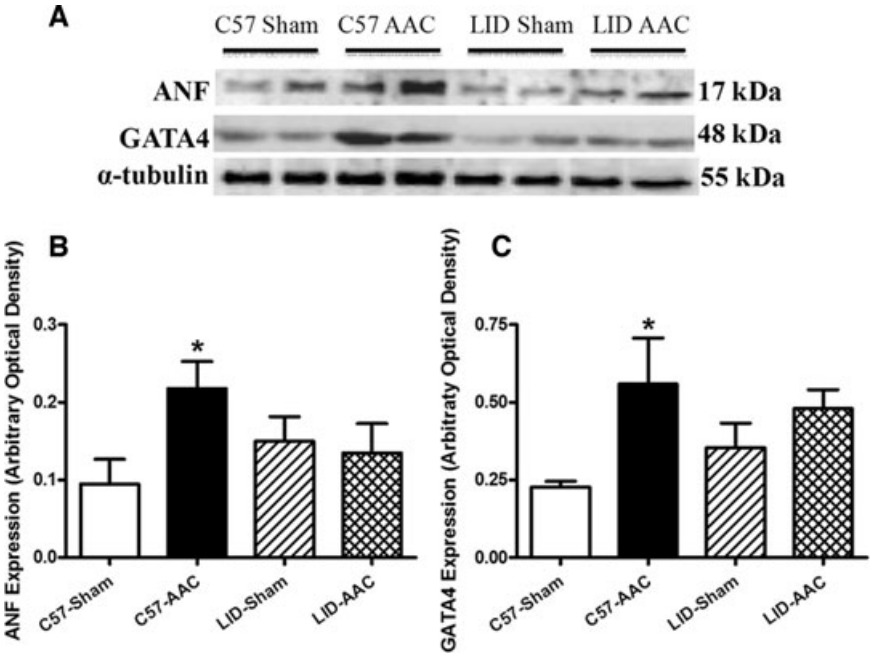

Fig. 4 Western blot analysis of the hypertrophic markers ANF and GATA4 from C57 and LID mice hearts with sham or AAC treatment. (**A**) Representative gel blots depicting expression of ANF, GATA4 and α-tubulin (loading control) using specific antibodies; (**B**) ANF and (**C**) GATA4. Mean ± S.E.M., $n = 6$/group, $^{*}P < 0.05$ *versus* C57-sham group.

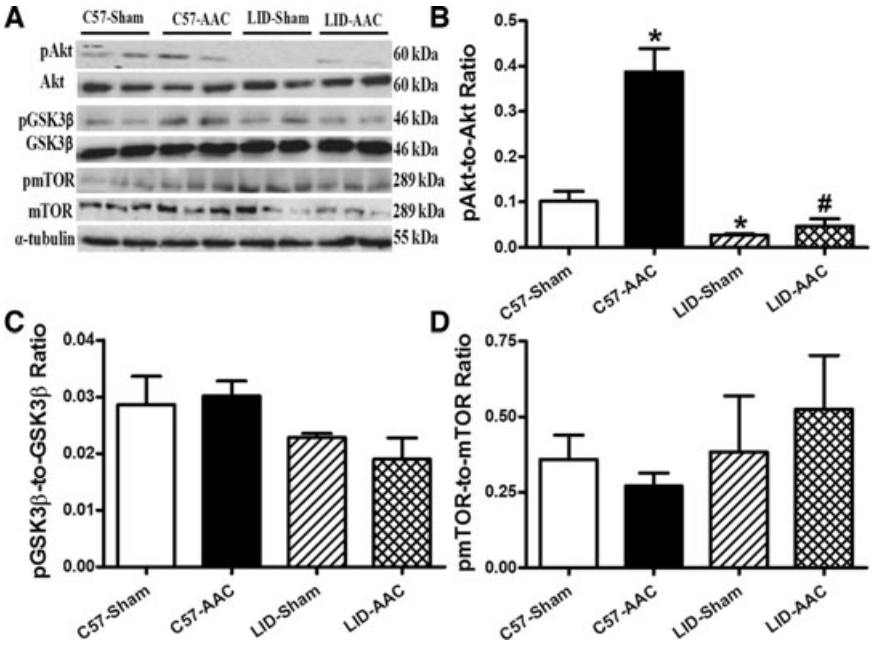

Fig. 5 Western blot analysis of pan and phosphorylated Akt, GSK-3β, and mTOR in myocardium from C57 and LID mice with either sham or AAC treatment. (**A**) Representative gel blots depicting pan and phosphorylated Akt, GSK-3β and mTOR (α-tubulin as loading control) using specific antibodies; (**B**) pAkt-to-Akt ratio; (**C**) pGSK-3β-to-GSK-3β ratio and (**D**) pmTOR-to-mTOR ratio; mean ± S.E.M., $n = 6$ hearts/group, $^{*}P < 0.05$ *versus* C57-sham group, $^{\#}P < 0.05$ *versus* C57-AAC group.

related to increased interstitial fibrosis, resulting in an adaptive increase in single cardiomyocyte function. Nonetheless, dampened cardiomyocyte contractile capacity was also noted in hypertrophic mice [36]. Such disparity in cardiomyocyte function may be due to the difference in the duration of cardiac hypertrophy and difference in maladaptive *versus* adaptive hypertrophy (such as in our current study). Here we failed to observe any change in intracellular Ca^{2+} handling (baseline, peak intracellular Ca^{2+} and intracellular Ca^{2+} clearance) along with stimulus frequency response in cardiomyocytes from pressure overloaded hearts, thus not favouring a major role of Ca^{2+} homeostasis in pressure overload or IGF-1 deficiency-induced cardiac mechanical response.

© 2011 The Authors
Journal of Cellular and Molecular Medicine © 2011 Foundation for Cellular and Molecular Medicine/Blackwell Publishing Ltd

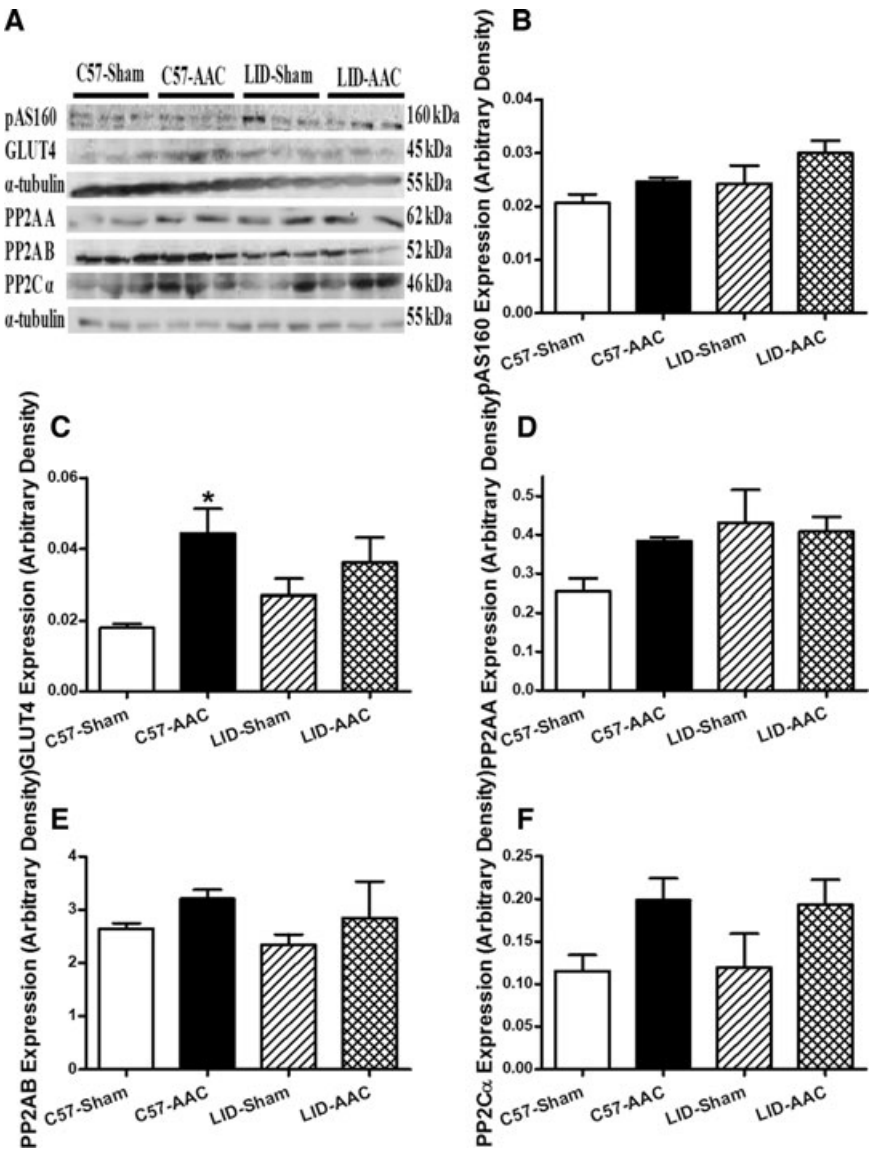

Fig. 6 Western blot analysis of phosphorylated AS160 (pAS160), GLUT4, PP2AA, PP2AB and PP2Cα in myocardium from C57 and LID mice with sham or AAC treatment. (**A**) Representative gel blots depicting pAS160, GLUT4, PP2AA, PP2AB, PP2Cα and α-tubulin (loading control) using specific antibodies; (**B**) pAS160; (**C**) GLUT4; (**D**) PP2AA; (**E**) PP2AB and (**F**) PP2Cα. Mean ± S.E.M., $n = 6$ hearts per group, $^*P < 0.05$ *versus* C57-sham group.

Evaluation of intracellular Ca^{2+} handling from several animal models of cardiac hypertrophy and heart failure has yielded somewhat contradictory findings. Intracellular Ca^{2+} levels were found to be decreased [37] or elevated [38] in hypertrophic cardiomyocytes. Moreover, prolonged intracellular Ca^{2+} transients were reported in models of advanced cardiac hypertrophy [39, 40], in line with the decreased sarcoplasmic reticulum Ca^{2+} uptake and reduced Ca^{2+} release in advanced hypertrophic or failing hearts [41, 42]. Therefore, alteration in sarcoplasmic reticulum function at various stages of cardiac hypertrophy may play a role in intracellular Ca^{2+} handling under pressure overload although further study is warranted.

IGF-1 plays a rather unique role in the regulation of cardiac geometry and contractile function [11, 20]. Severely dysfunctional myocardium following myocardial infarction is capable of undergoing hypertrophy associated with improved contractile function with IGF-1 treatment, favouring a beneficial effect of the growth factor [19]. To the contrary, elevated circulating IGF-1 levels are seen in acromegalic patients with cardiac hypertrophy [43]. This is consistent with the pro-hypertrophic response of IGF-1 in cardiac gene expression, the effect of which may be attenuated by IGF binding protein-3 [44]. Thus a contemporary mechanism seems to be present for IGF-1-induced cardiac regulation with an initial adaptive hypertrophy followed the undesirable transition from

© 2011 The Authors

Journal of Cellular and Molecular Medicine © 2011 Foundation for Cellular and Molecular Medicine/Blackwell Publishing Ltd

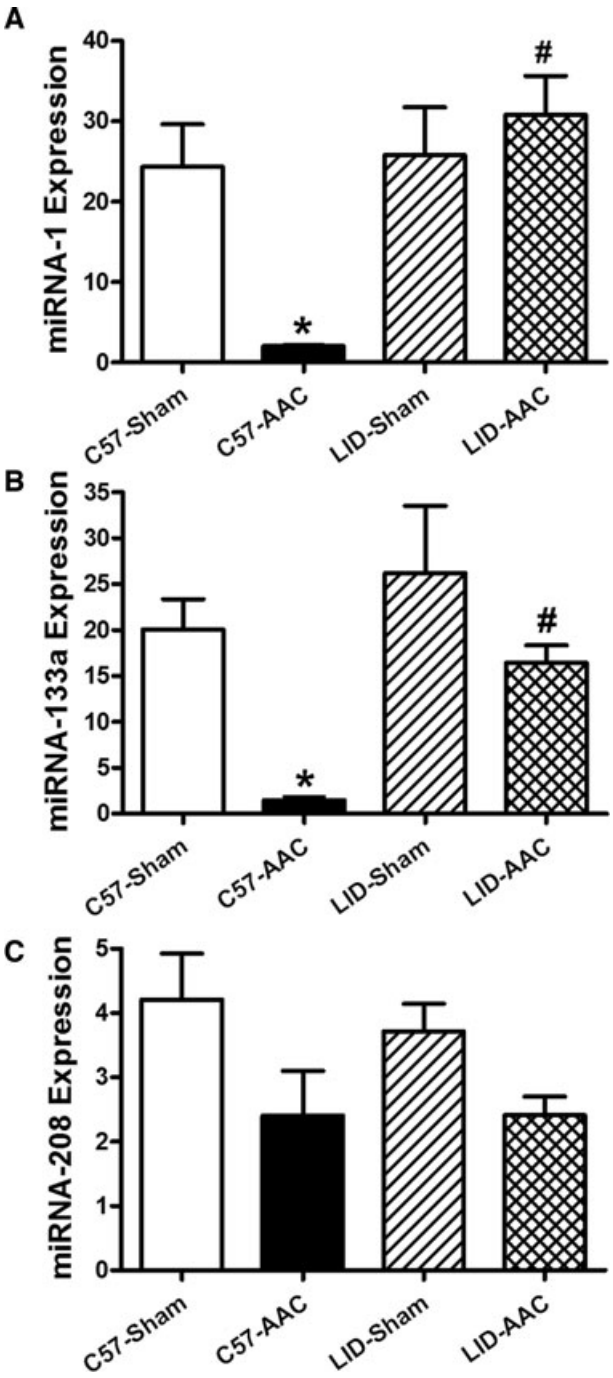

Fig. 7 Quantitative real time-PCR analysis of miRNA-1, miRNA-133a and miRNA-208 in ventricles from C57 and LID mice with sham or AAC treatment. (**A**) miRNA-1; (**B**) miRNA-133a and (**C**) miRNA-208a; mean ± S.E.M., $n = 6$ hearts per group, $^{*}P < 0.05$ *versus* C57-sham group, $^{\#}P < 0.05$ *versus* C57-AAC group.

hypertrophy to heart failure. Distinct signalling machineries in IGF-1-induced hypertrophy have been reported including Akt and its downstream signalling molecules mTOR and GSK-3β [19–21]. On the other hand, the essential hypertrophic signal calcineurin was not found to participate in IGF-1-induced hypertrophy [21]. More recent study in myocardium reported that eccentric cardiac hypertrophy is associated with altered IGF-1-mediated regulation of potassium channels through mitogen-activated protein kinase and Akt signalling cascades [26]. Our findings favour a role of hyperactivated Akt signal along with up-regulated GLUT4 expression (although not mTOR, GSK-3β, AS160 signalling) in AAC- or IGF-1 deficiency-induced hypertrophic responses. Our observations of unchanged expression of PP2AA, PP2AB and PP2Cα did not favour any role of protein phosphatase in AAC or IGF-1 deficiency-induced changes in Akt phosphorylation. Last but not least, it is worth mentioning that IGF-1 may offer its cardiac benefit through non-IGF-1 receptor-mediated mechanisms such as anti-oxidation [20].

MiRs are complementary with specific mRNAs to down-regulate post-transcriptional gene expression through suppressing translation or promoting mRNA degradation [15]. MiRs are transcribed as long primary transcripts (pri-miRs) before undergoing sequential steps to mature. First, the nuclear processing of the pri-miRs into stem-loop precursors of ~70 nucleotides (pre-miRs), and the cytoplasmic processing of pre-miRs into mature miRs [45]. MiRs are deemed key factors for cardiac development and proliferation. In particular, miR-1 and miR-133a are considered to be muscle specific [46]. For example, MiR-1 inhibits myocyte proliferation and cardiac development [47]. The pressure overload-induced cardiac hypertrophy displays cardiac pathology with a global change in the gene expression profile *via* some unknown mechanism(s). It was reported that the muscle-specific miR molecule miR-1 was down-regulated in the heart at the onset of pressure overload [48]. It is possible that depressed miR-1 level was sufficient to induce gene expression changes thus underscoring cardiac hypertrophy. Our data revealed that miR-1 and miR-133a levels were decreased in C57 but not IGF-1-deficient hypertrophic model. Furthermore, transfection with miR-1 and miR-133a alleviates IGF-1-induced cardiomyocyte hypertrophy, indicating that IGF-1 deficiency may rescue cardiac hypertrophy through preserved miR-1 and miR-133a levels. MiR-1/miR-133a was found clustered together, and the cluster are transcribed from non-coding regions on mouse chromosome 2 [49]. Given that our data failed to identify any change in miR-208 level following AAC, our results favour the notion that the miR-1/miR-133a cluster may participate in the IGF-1-induced cardiac hypertrophy. Although it is beyond the scope of our current study, it is imperative to delineate the regulatory role of IGF-1 on miRs. Although recent data suggested a direct role of IGF-1 in the regulation of miRs through transcriptional regulation of Foxo3a [48], possible contribution of myocardin, a regulator of miRNA, to the IGF-1 response [50, 51], should not be discounted.

© 2011 The Authors
Journal of Cellular and Molecular Medicine © 2011 Foundation for Cellular and Molecular Medicine/Blackwell Publishing Ltd

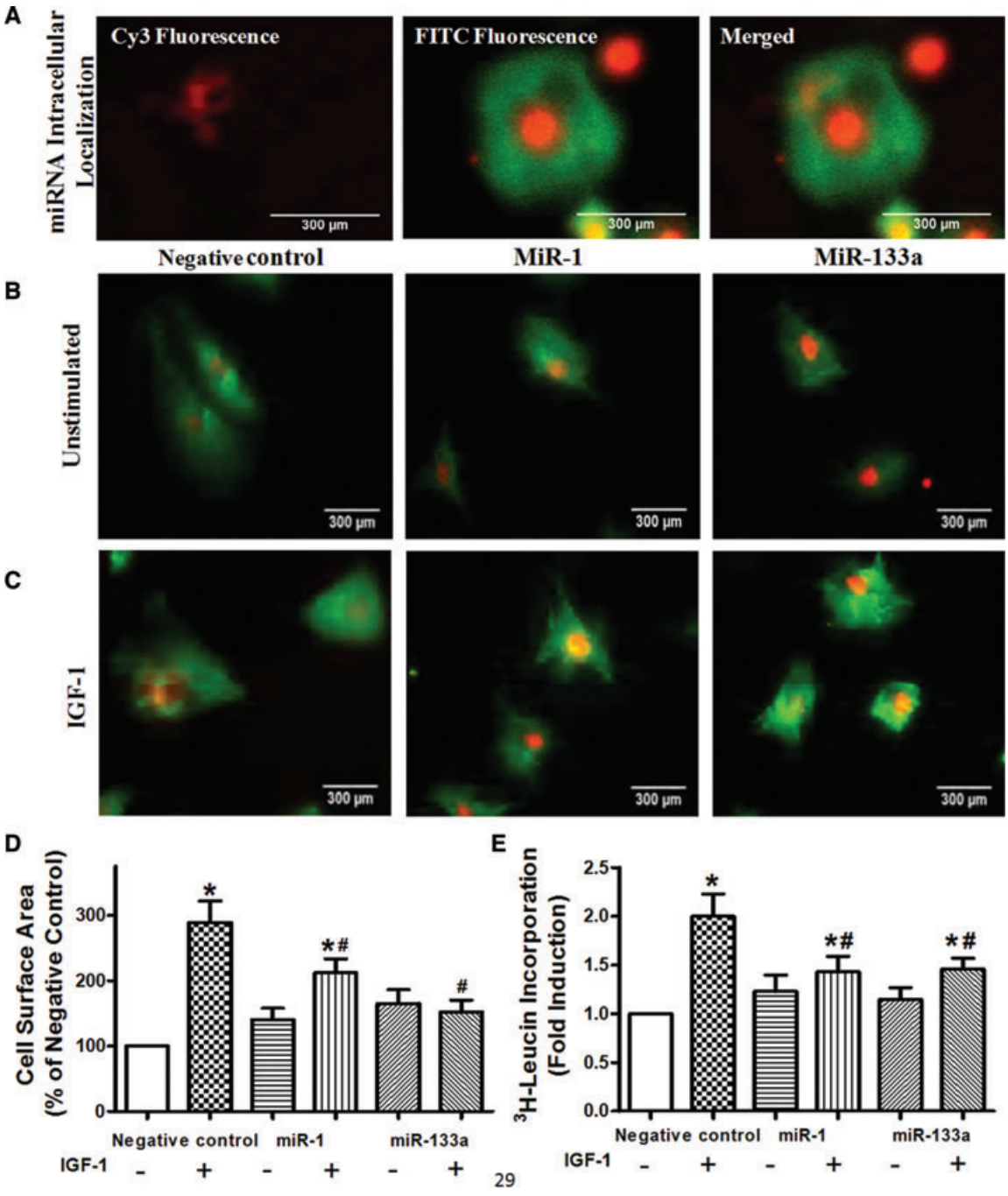

Fig. 8 Effect of overexpression of miRNA-1 and miRNA-133a on IGF-1-induced hypertrophic response in NRCMs. (**A**) Intracellular localization of miRNA (Cy3 fluorescence) detected by a Nikon Eclipse TE300 microscope (left panel). Middle panel displays image of cells (FITC fluorescence) with the right panel exhibiting the overlay depicting Cy3 fluorescence in one NRCM. (**B**) Representative images of NRCMs transfected with negative control miRNA, miRNA-1 and miRNA-133a for 48 hrs in the absence of IGF-1 (unstimulated). (**C**) Representative images of NRCMs transfected with negative control miRNA, miRNA-1 and miRNA-133a in the presence of IGF-1 (30 ng/ml) for 48 hrs. Cells were stained with the anti-α-actin antibody to confirm cardiomyocyte purity. (**D**) Cell surface area of NRCMs overexpressing negative control miRNA, miRNA-1 and miRNA-133a treated with or without IGF-1 (30 ng/ml) for 48 hrs and (**E**) ^{3}H-Leucine incorporation in NRCMs overexpressing negative control miRNA, miRNA-1 or miRNA-133a treated with or without IGF-1 (30 ng/ml) for 48 hrs; mean ± S.E.M., $n = 6$ independent experiments per group, $^{*}P < 0.05$ *versus* negative control group in the absence of IGF-1, $^{\#}P < 0.05$ *versus* corresponding IGF-1-stimulated negative control group.

© 2011 The Authors

Journal of Cellular and Molecular Medicine © 2011 Foundation for Cellular and Molecular Medicine/Blackwell Publishing Ltd

In summary, our study offered evidence for the first time that IGF-1 deficiency mitigated cardiac hypertrophic remodelling and myocardial contractile change following pressure overload-induced cardiac hypertrophy. Meanwhile, IGF-1 deficiency alleviated up-regulated hypertrophic markers, Akt phosphorylation and GLUT4 following pressure overload. More importantly, such geometric, mechanical and protein alterations under IGF-1 deficiency and AAC were mirrored by changes in miR-1 and miR-133a. The possible involvement of miRs in IGF-1 deficiency-elicited beneficial effect against cardiac hypertrophy received some compelling support where overexpression of miR-1 and miR-133a blunt IGF-1-induced cardiomyocyte hypertrophy. These data support the hypothesis that IGF-1 deficiency is capable of retarding AAC-induced cardiac hypertrophy and contractile dysregulation *via* rescuing the down-regulated miR-1 and miR-133a levels.

Acknowledgement

The authors thank Dr. Heng Ma for his generous assistance. This work was presented in abstract form at the American Heart Association Scientific Session 2009 in Orlando.

Funding source: This work was supported in part by NIH/NCRR 5P20 RR016474.

Conflict of interest

The authors confirm that there are no conflicts of interest.

References

1. **Berk BC, Fujiwara K, Lehoux S**. ECM remodeling in hypertensive heart disease. *J Clin Invest*. 2007; 117: 568–75.
2. **Chen F, Kook H, Milewski R, *et al.*** Hop is an unusual homeobox gene that modulates cardiac development. *Cell*. 2002; 110: 713–23.
3. **Heineke J, Molkentin JD**. Regulation of cardiac hypertrophy by intracellular signalling pathways. *Nat Rev Mol Cell Biol*. 2006; 7: 589–600.
4. **Molkentin JD, Lu JR, Antos CL, *et al.*** A calcineurin-dependent transcriptional pathway for cardiac hypertrophy. *Cell*. 1998; 93: 215–28.
5. **Naga Prasad SV, Esposito G, Mao L, *et al.*** Gbetagamma-dependent phosphoinositide 3-kinase activation in hearts with *in vivo* pressure overload hypertrophy. *J Biol Chem*. 2000; 275: 4693–8.
6. **Antos CL, McKinsey TA, Frey N, *et al.*** Activated glycogen synthase-3 beta suppresses cardiac hypertrophy *in vivo*. *Proc Natl Acad Sci USA*. 2002; 99: 907–12.
7. **Zhang CL, McKinsey TA, Chang S, *et al.*** Class II histone deacetylases act as signal-responsive repressors of cardiac hypertrophy. *Cell*. 2002; 110: 479–88.
8. **Zhang T, Johnson EN, Gu Y, *et al.*** The cardiac-specific nuclear delta(B) isoform of Ca2+/calmodulin-dependent protein kinase II induces hypertrophy and dilated cardiomyopathy associated with increased protein phosphatase 2A activity. *J Biol Chem*. 2002; 277: 1261–7.
9. **Paradis P, Dali-Youcef N, Paradis FW, *et al.*** Overexpression of angiotensin II type I receptor in cardiomyocytes induces cardiac hypertrophy and remodeling. *Proc Natl Acad Sci USA*. 2000; 97: 931–6.
10. **Bueno OF, De Windt LJ, Lim HW, *et al.*** The dual-specificity phosphatase MKP-1 limits the cardiac hypertrophic response *in vitro* and *in vivo*. *Circ Res*. 2001; 88: 88–96.
11. **Delafontaine P, Brink M**. The growth hormone and insulin-like growth factor 1 axis in heart failure. *Ann Endocrinol*. 2000; 61: 22–6.
12. **Yang R, Bunting S, Gillett N, *et al.*** Growth hormone improves cardiac performance in experimental heart failure. *Circulation*. 1995; 92: 262–7.
13. **Care A, Catalucci D, Felicetti F, *et al.*** MicroRNA-133 controls cardiac hypertrophy. *Nat Med*. 2007; 13: 613–8.
14. **Ikeda S, He A, Kong SW, *et al.*** MicroRNA-1 negatively regulates expression of the hypertrophy-associated calmodulin and Mef2a genes. *Mol Cell Biol*. 2009; 29: 2193–204.
15. **Pasquinelli AE, Reinhart BJ, Slack F, *et al.*** Conservation of the sequence and temporal expression of let-7 heterochronic regulatory RNA. *Nature*. 2000; 408: 86–9.
16. **Lewis BP, Burge CB, Bartel DP**. Conserved seed pairing, often flanked by adenosines, indicates that thousands of human genes are microRNA targets. *Cell*. 2005; 120: 15–20.
17. **Baskerville S, Bartel DP**. Microarray profiling of microRNAs reveals frequent coexpression with neighboring miRNAs and host genes. *RNA*. 2005; 11: 241–7.
18. **van Rooij E, Sutherland LB, Qi X, *et al.*** Control of stress-dependent cardiac growth and gene expression by a microRNA. *Science*. 2007; 316: 575–9.
19. **Duerr RL, Huang S, Miraliakbar HR, *et al.*** Insulin-like growth factor-1 enhances ventricular hypertrophy and function during the onset of experimental cardiac failure. *J Clin Invest*. 1995; 95: 619–27.
20. **Ren J, Samson WK, Sowers JR**. Insulin-like growth factor I as a cardiac hormone: physiological and pathophysiological implications in heart disease. *J Mol Cell Cardiol*. 1999; 31: 2049–61.
21. **Rommel C, Bodine SC, Clarke BA, *et al.*** Mediation of IGF-1-induced skeletal myotube hypertrophy by PI(3)K/Akt/mTOR and PI(3)K/Akt/GSK3 pathways. *Nat Cell Biol*. 2001; 3: 1009–13.
22. **Funai K, Cartee GD**. Inhibition of contraction-stimulated AMP-activated protein kinase inhibits contraction-stimulated increases in PAS-TBC1D1 and glucose transport without altering PAS-AS160 in rat skeletal muscle. *Diabetes*. 2009; 58: 1096–104.
23. **Li Q, Yang X, Sreejayan N, *et al.*** Insulin-like growth factor I deficiency prolongs survival and antagonizes paraquat-induced cardiomyocyte dysfunction: role of oxidative stress. *Rejuvenation Res*. 2007; 10: 501–12.
24. **Yakar S, Liu JL, Stannard B, *et al.*** Normal growth and development in the absence of hepatic insulin-like growth factor I. *Proc Natl Acad Sci USA*. 1999; 96: 7324–9.
25. **Wu JH, Hagaman J, Kim S, *et al.*** Aortic constriction exacerbates atherosclerosis and induces cardiac dysfunction in mice

© 2011 The Authors
Journal of Cellular and Molecular Medicine © 2011 Foundation for Cellular and Molecular Medicine/Blackwell Publishing Ltd

lacking apolipoprotein E. *Arterioscler Thromb Vasc Biol*. 2002; 22: 469–75.

26. **Teos LY, Zhao A, Alvin Z, *et al.*** Basal and IGF-I-dependent regulation of potassium channels by MAP kinases and PI3-kinase during eccentric cardiac hypertrophy. *Am J Physiol Heart Circ Physiol*. 2008; 295: H1834–45.
27. **Doser TA, Turdi S, Thomas DP, *et al.*** Transgenic overexpression of aldehyde dehydrogenase-2 rescues chronic alcohol intake-induced myocardial hypertrophy and contractile dysfunction. *Circulation*. 2009; 119: 1941–9.
28. **O'Connell RM, Taganov KD, Boldin MP, *et al.*** MicroRNA-155 is induced during the macrophage inflammatory response. *Proc Natl Acad Sci USA*. 2007; 104: 1604–9.
29. **von Harsdorf R, Li PF, Dietz R**. Signaling pathways in reactive oxygen species-induced cardiomyocyte apoptosis. *Circulation*. 1999; 99: 2934–41.
30. **Barbier J, Dutertre M, Bittencourt D, *et al.*** Regulation of H-ras splice variant expression by cross talk between the p53 and nonsense-mediated mRNA decay pathways. *Mol Cell Biol*. 2007; 27: 7315–33.
31. **Zhu H, McElwee-Witmer S, Perrone M, *et al.*** Phenylephrine protects neonatal rat cardiomyocytes from hypoxia and serum deprivation-induced apoptosis. *Cell Death Differ*. 2000; 7: 773–84.
32. **Oceandy D, Pickard A, Prehar S, *et al.*** Tumor suppressor Ras-association domain family 1 isoform A is a novel regulator of cardiac hypertrophy. *Circulation*. 2009; 120: 607–16.
33. **Fritton JC, Emerton KB, Sun H, *et al.*** Growth hormone protects against ovariectomy-induced bone loss in states of low circulating insulin-like growth factor (IGF-1). *J Bone Miner Res*. 2010; 25: 235–46.
34. **Callis TE, Pandya K, Seok HY, *et al.*** MicroRNA-208a is a regulator of cardiac hypertrophy and conduction in mice. *J Clin Invest*. 2009; 119: 2772–86.
35. **Hunter JJ, Chien KR**. Signaling pathways for cardiac hypertrophy and failure. *N Engl J Med*. 1999; 341: 1276–83.
36. **Takeishi Y, Ping P, Bolli R, *et al.*** Transgenic overexpression of constitutively active protein kinase C epsilon causes concentric cardiac hypertrophy. *Circ Res*. 2000; 86: 1218–23.
37. **Siri FM, Krueger J, Nordin C, *et al.*** Depressed intracellular calcium transients and contraction in myocytes from hypertrophied and failing guinea pig hearts. *Am J Physiol*. 1991; 261: H514–30.
38. **Pearce PC, Hawkey C, Symons C, *et al.*** Role of calcium in the induction of cardiac hypertrophy and myofibrillar disarray. Experimental studies of a possible cause of hypertrophic cardiomyopathy. *Br Heart J*. 1985; 54: 420–7.
39. **Bailey BA, Houser SR**. Calcium transients in feline left ventricular myocytes with hypertrophy induced by slow progressive pressure overload. *J Mol Cell Cardiol*. 1992; 24: 365–73.
40. **Perreault CL, Shannon RP, Komamura K, *et al.*** Abnormalities in intracellular calcium regulation and contractile function in myocardium from dogs with pacing-induced heart failure. *J Clin Invest*. 1992; 89: 932–8.
41. **Brillantes AM, Allen P, Takahashi T, *et al.*** Differences in cardiac calcium release channel (ryanodine receptor) expression in myocardium from patients with end-stage heart failure caused by ischemic *versus* dilated cardiomyopathy. *Circ Res*. 1992; 71: 18–26.
42. **Limas CJ, Cohn JN**. Defective calcium transport by cardiac sarcoplasmic reticulum in spontaneously hypertensive rats. *Circ Res*. 1977; 40: I62–9.
43. **Page MD, Millward ME, Taylor A, *et al.*** Long-term treatment of acromegaly with a long-acting analogue of somatostatin, octreotide. *Q J Med*. 1990; 74: 189–201.
44. **Ito H, Hiroe M, Hirata Y, *et al.*** Insulin-like growth factor-I induces hypertrophy with enhanced expression of muscle specific genes in cultured rat cardiomyocytes. *Circulation*. 1993; 87: 1715–21.
45. **Lee Y, Jeon K, Lee JT, *et al.*** MicroRNA maturation: stepwise processing and subcellular localization. *EMBO J*. 2002; 21: 4663–70.
46. **Lagos-Quintana M, Rauhut R, Yalcin A, *et al.*** Identification of tissue-specific microRNAs from mouse. *Curr Biol*. 2002; 12: 735–9.
47. **Zhao Y, Samal E, Srivastava D**. Serum response factor regulates a muscle-specific microRNA that targets Hand2 during cardiogenesis. *Nature*. 2005; 436: 214–20.
48. **Elia L, Contu R, Quintavalle M, *et al.*** Reciprocal regulation of microRNA-1 and insulin-like growth factor-1 signal transduction cascade in cardiac and skeletal muscle in physiological and pathological conditions. *Circulation*. 2009; 120: 2377–85.
49. **Chen JF, Mandel EM, Thomson JM, *et al.*** The role of microRNA-1 and microRNA-133 in skeletal muscle proliferation and differentiation. *Nat Genet*. 2006; 38: 228–33.
50. **Liu ZP, Wang Z, Yanagisawa H, *et al.*** Phenotypic modulation of smooth muscle cells through interaction of Foxo4 and myocardin. *Dev Cell*. 2005; 9: 261–70.
51. **Xing W, Zhang TC, Cao D, *et al.*** Myocardin induces cardiomyocyte hypertrophy. *Circ Res*. 2006; 98: 1089–97.

© 2011 The Authors
Journal of Cellular and Molecular Medicine © 2011 Foundation for Cellular and Molecular Medicine/Blackwell Publishing Ltd